SLAC–PUB–7370
March 1997

A MØLLER POLARIMETER FOR HIGH ENERGY ELECTRON BEAMS *

H. R. Band, G. Mitchell, R. Prepost, T. Wright
University of Wisconsin, Madison, WI 53706
Stanford Linear Accelerator Center, Stanford University, Stanford, CA 94309

Abstract

A single arm Møller polarimeter used to measure the longitudinal beam polarization of the 48 GeV electron beam for SLAC fixed target experiment E–154 is described. The polarimeter utilizes an array of silicon strip detectors and a dipole magnetic spectrometer to detect Møller scattered electrons from magnetized Fe-Co alloy target foils. The details of the foil polarization measurements and analysis technique are discussed. The high statistical precision of the Møller data and the stablity of the SLAC polarized source made precise studies of the systematic errors in the analysis possible. An overall systematic error of 2.7 % is assigned to the beam polarization determination.

Submitted to *Nuclear Instruments and Methods in Physics Research Section A*

*Work supported by Department of Energy contract DE–AC03–76SF00515 and DE–AC02–76ER00881.

A MØLLER POLARIMETER FOR HIGH ENERGY ELECTRON BEAMS

H. R. Band, [1] G. Mitchell, R. Prepost, T. Wright

University of Wisconsin
Madison, WI 53706

Abstract

A single arm Møller polarimeter used to measure the longitudinal beam polarization of the 48 GeV electron beam for SLAC fixed target experiment E–154 is described. The polarimeter utilizes an array of silicon strip detectors and a dipole magnetic spectrometer to detect Møller scattered electrons from magnetized Fe-Co alloy target foils. The details of the foil polarization measurements and analysis technique are discussed. The high statistical precision of the Møller data and the stablity of the SLAC polarized source made precise studies of the systematic errors in the analysis possible. An overall systematic error of 2.7 % is assigned to the beam polarization determination.

1 Introduction

The fixed target program at the Stanford Linear Accelerator Center (SLAC) currently consists of a series of experiments to measure nucleon spin dependent structure functions. For each of these experiments (E-142, E-143, E-154, and E-155) the beam polarization was measured using the technique of Møller polarimetry[1]. This paper describes in detail the single arm Møller polarimeter which was used for the recent SLAC E-154 experiment.

Section 2 gives the kinematic, cross-section, and asymmetry expressions required to analyze Møller scattering data. Section 3 describes the details of the polarimeter design including the detector, magnetic spectrometer, and magnetic foil targets. Section 4 briefly describes aspects of the experimental conditions while Section 5 contains a detailed discussion of how the beam

[1] Corresponding author. Tel. 415-926-2655, fax 415-926-2923, e-mail hrb@slac.stanford.edu.

polarization is extracted from the Møller scattering data. Systematic error considerations are discussed in Section 6.

2 Møller Scattering

The details of spin dependent Møller scattering have been discussed by many authors. Only a brief description is presented here. The cross section for spin dependent elastic electron-electron scattering (Møller scattering [2]) is given by:

$$d\sigma/d\Omega = (d\sigma_0/d\Omega)\ (1 + \sum_{i,j} P_{\rm B}^i A_{ij} P_{\rm T}^j)$$

where $P_{\rm B}^i$ are the components of the beam polarization and $P_{\rm T}^j$ are the components of the target polarization. The z axis is along the beam direction and the y axis is chosen normal to the scattering plane. The cross section is given by the unpolarized cross section, $d\sigma_0/d\Omega$ and the asymmetry terms A_{ij}. If $P_{\rm T}$ is independently known, the above expression may be used to determine the beam polarization $P_{\rm B}$.

To lowest order, the fully relativistic unpolarized laboratory cross section is given by:

$$(d\sigma_0/d\Omega)_{\rm L} = \left[\frac{\alpha(1+\cos\theta_{\rm CM})(3+\cos^2\theta_{\rm CM})}{2m_e \sin^2\theta_{\rm CM}}\right]^2 .$$

Here $\theta_{\rm CM}$ is the center-of-mass scattering angle, m_e is the electron mass, and α is the fine structure constant. For the measurement of longitudinal polarization with a longitudinally polarized target foil, the only relevant asymmetry term is A_{zz}, given by:

$$A_{zz} = -\frac{(7+\cos^2\theta_{\rm CM})\sin^2\theta_{\rm CM}}{(3+\cos^2\theta_{\rm CM})^2} .$$

The asymmetry maximum is at $\theta_{\rm CM} = 90^\circ$ where the unpolarized laboratory cross section is 0.179 b/sr and $A_{zz} = -7/9$.

Møller polarimeters typically utilize thin ferromagnetic foils as the polarized electron target. The distinction between the free target electrons of the previous formulae and the bound atomic electrons of the physical target was ignored until Levchuk [3] pointed out that the analyzing power of Møller polarimeters may have significant corrections due to orbital motion of the target

foil electrons. Atomic electrons have shell dependent momentum distributions. Electrons in the outer shells have small momenta (≤ 5 KeV/c) but those from inner shells have momenta up to 100 KeV/c. Although small compared to a beam energy of 48 GeV, these momenta are not small compared to the electron rest mass and can alter the center of mass energy by as much as 20%.

The momentum and laboratory scattering angle of Møller scattered electrons are functions of $\theta_{\rm CM}$, m_e, the beam energy $E_{\rm b}$, and the component of the target electron momentum along the beam direction $p_{\rm z}^{\rm t}$[4]:

$$p_{\rm lab} = \frac{E_{\rm b}}{2}(1+\cos\theta_{\rm CM})$$

$$\theta_{\rm lab}^2 = 2m_e\left[\frac{1}{p_{\rm lab}} - \frac{1}{E_{\rm b}}\right]\left[1-\frac{p_{\rm z}^{\rm t}}{m_e}\right] = (\theta_{\rm lab}^0)^2\left[1-\frac{p_{\rm z}^{\rm t}}{m_e}\right].$$

The laboratory angle with no target motion is denoted by $\theta_{\rm lab}^0$. The laboratory momentum $p_{\rm lab}$ is independent of the target motion, while $\theta_{\rm lab}$ varies as the square root of the target motion correction to the center of mass energy. The probability of observing a Møller scatter for an arbitrary $\theta_{\rm CM}$ and $E_{\rm b}$ (fixed $p_{\rm lab}$) is plotted versus lab angle for polarized and unpolarized electrons in Fig. 1. The horizontal axis is in units of $\theta_{\rm lab}^0$. As seen in Fig. 1 scatters from polarized target electrons have a narrower angular spread due to target momenta than scatters from all target electrons. The expected Møller asymmetry thus varies over the Møller scattering elastic peak. Inclusion of this effect has been shown to modify the analyzing power of Møller polarimeters by up to 15% [3,4] depending on the exact geometry of the polarimeter.

3 Polarimeter Design

The polarimeter consists of polarized target foils, a mask to define the azimuthal and vertical acceptance, a magnet to momentum analyze the scattered electrons, and detectors to measure the scattering rate. The E–154 polarimeter is an evolution of previous End Station A (ESA) Møller Polarimeters[1] and utilizes many ideas and components of previous designs. The top view (bend plane) and side view (scattering plane) of the polarimeter are shown in Fig. 2.

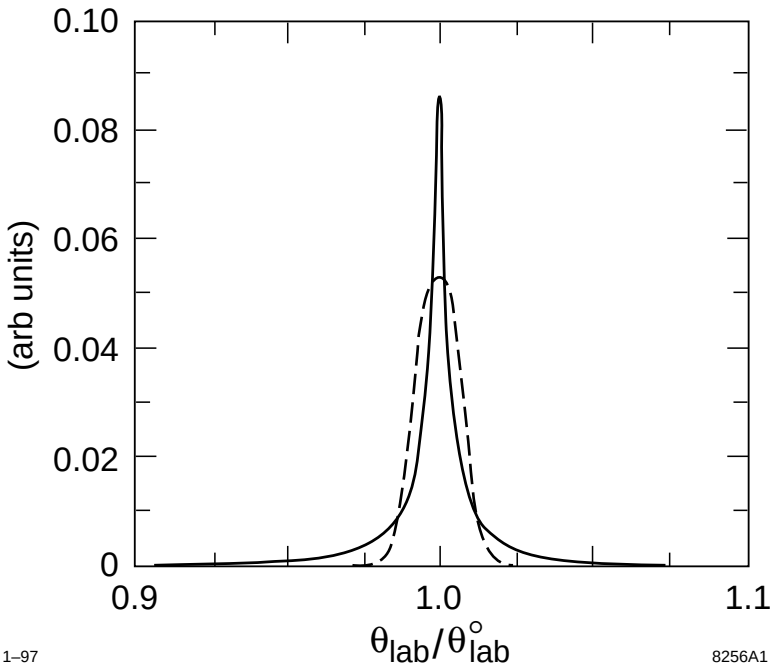

Fig. 1. The calculated distribution of laboratory scattering angles for Møller scattering from M shell polarized target electrons (dashed) and from all target electrons (solid) at fixed $\theta_{\rm CM}$ and $E_{\rm b}$. The horizontal axis is in units of the nominal scattering angle $\theta^0_{\rm lab}$ expected with no electron orbital motion.

3.1 Target

The polarized target was originally constructed for a previous SLAC experiment[5]. The target was refurbished with new foils, pickup coils, and a stepping motor for positioning the foils. The target foils are made of Vacoflux [1] , an alloy of 49% Co, 49% Fe, and 2% Va by weight.

Six foils of approximate thicknesses 20(2), 30, 40(2), and 154 μm were installed. Data were taken with all of the foils. The foils were magnetized to near saturation by Helmholtz coils providing 100 gauss at the target center. The polarity of the coils was typically reversed between Møller data runs to alternate the sign of the foil polarization and to minimize systematic errors. More than half of the data runs used one of the 40 μm foils. The remaining runs were spread over the other five foils.

The foils, typically 3 cm wide by 35 cm long, are threaded through pickup coils made from 500 turns of 30 gauge wire and stretched over a window frame mounted at 20.7° with respect to the beam. The window frame can be positioned to center any target foil on the beam line. The pickup coils are

[1] Vacuumschmelze GmbH, Hanau, Germany

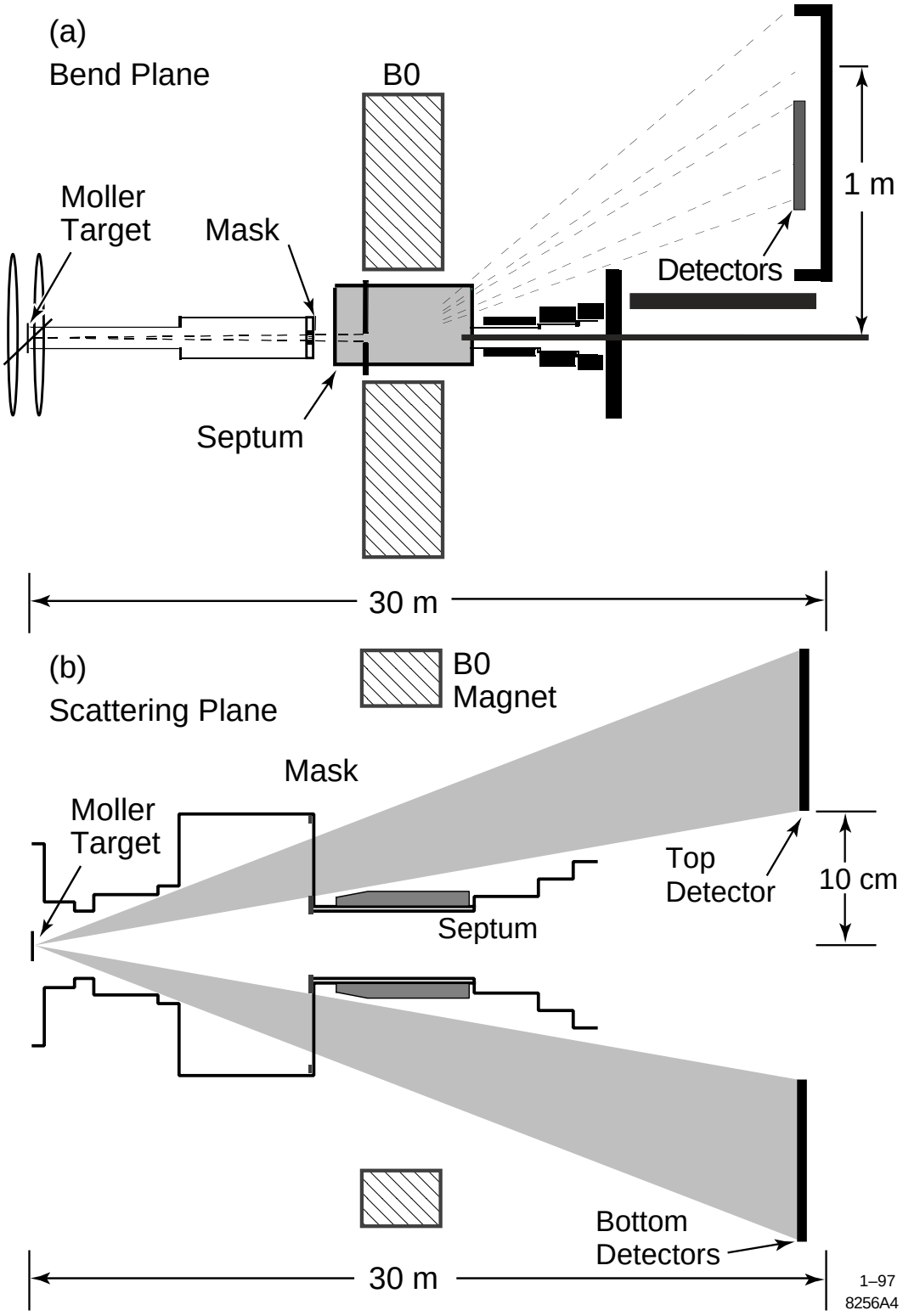

Fig. 2. Top(a) and side(b) views of the E–154 Møller Polarimeter showing the Møller target, mask, magnet, septum and top and bottom detectors.

mounted rigidly to a bar which slides over the window frame. Under data taking conditions the bar and pickup coils are pushed to the edge of the frame well out of the path of the beam. During foil polarization measurements the target chamber is opened and the bar and pickup coils are slid to the foil center. This arrangement allows for foil measurements without remounting the foils and has yielded stable and repeatable measurements.

3.2 Foil Polarization

The polarization P_{T} of the target electrons was determined from the relation:

$$P_{\mathrm{T}} = \frac{M}{n_e \mu_{\mathrm{B}}} \times \left(\frac{g' - 1}{g'}\right) \times \left(\frac{g_e}{g_e - 1}\right) ,$$

where M is the bulk magnetization in the foil, n_e is the electron density, $g_e = 2.002319$ is the free electron g factor, and $\mu_{\mathrm{B}} = 9.273 \times 10^{-21}$ G-cm^3 is the Bohr magneton. The factor involving the magnetomechanical ratio (g') is needed to make a correction for the orbital contribution to the magnetization. A measurement of $g' = 1.916 \pm 0.002$ by Scott and Sturner[6] for an alloy of 50% Fe and 50% Co is used with the assumption that the vanadium in the foils does not alter g'.[7] We have increased the g' error to 0.01 to reflect the uncertainties in the original and earlier measurements[8] and to reflect a possible uncertainty in the effect of the vanadium. Substituting into the above equation yields:

$$P_{\mathrm{T}} = \frac{M}{n_e \mu_{\mathrm{B}}} \times (0.9551 \pm 0.006).$$

The electron density can be calculated from $n_e = \rho N_{\mathrm{A}} < Z > / < A >$ where $< Z >$ and $< A >$ are the average atomic number and mass number of the Vacoflux alloy, N_{A} is Avogadro's number and ρ is the density of the foil. M is determined from the relation $4\pi M = B - H$.

3.3 Foil Magnetization Measurements

The measurement technique used a precise integrating voltmeter[2] (IVM) connected to a pickup coil placed around the foils. As the bipolar Helmholtz coil power supply swept the H field from –100 to +100 Gauss the IVM measured

[2] Schlumberger SI 7061

the integrated induced voltage. From Faraday's law the voltage integral can be related to the magnetic field B inside the foil through

$$\int \mathrm{Vdt} = 2 \times N_\mathrm{T} \times (A_\mathrm{foil} B + (A_\mathrm{coil} - A_\mathrm{foil}) H),$$

where A_foil and A_coil are the cross-section area of the foil and pickup coil respectively and N_T is the number of turns in the pickup coil. By repeating the measurement without the foil in place and subtracting the foil-out integral from the foil-in integral we find:

$$4\pi M = B - H = \frac{\int_\mathrm{in} \mathrm{Vdt} - \int_\mathrm{out} \mathrm{Vdt}}{2 \times N_\mathrm{T} \times A_\mathrm{foil}} \ .$$

Combining the equations for P_T and for M, and recognizing that the average foil density can be determined from the measured mass (m) , length (l) and area A_foil of the foil, the polarization can be determined from:

$$P_\mathrm{T} = (1.474 \pm 0.010) \times l \times \frac{(\int_\mathrm{in} \mathrm{Vdt} - \int_\mathrm{out} \mathrm{Vdt})}{m \times N_\mathrm{T}}.$$

where l is in cm , m in grams, and Vdt is measured in mV-s. These variables can be measured to better than 0.1% accuracy.

The foils were each measured with 5 ramps from –100 to +100 G and 5 ramps from +100 to –100 G. The spread of the data was used to compute the measurement error which was typically 0.05 to 0.10 %. The absolute calibration of the voltmeter was 0.001 mV-s. Since typical signals for foil-out integrals were 0.6 mV-s and for foil-in integrals were 2-4 mV-s, the relative error on $\int Vdt$ was no greater than 0.1%.

3.4 Foil Measurement Results

A systematic study of the magnetization measurements was made in which more than thirty foils 20, 30, 40, and 154 μm thick were measured at the nominal foil center and at $\pm 6, \pm 12$ mm from the center. Only one foil was mounted on the target frame at a time. All measurements were made with a 3 mm long pickup coil (500 turns). After correcting for the average length and mass of the foil, the spread of the measured polarization values was 1.5% for the 20 μm foils and 1.7% for the thicker foils. The spread in the measured polarizations along the length of a single foil were about 1.1%. Averaging the five measurements along the length of a single foil produced a more precise foil polarization with a smaller (0.9-1.3 %) spread than the individual measurements.

Foil Number	Foil thickness	Measured Polarization
1	154 μm	0.0828
2	30 μm	0.0819
3	40 μm	0.0820
4	20 μm	0.0812
5	20 μm	0.0811
6	40 μm	0.0822

Table 1
Polarizations of the E–154 target foils.

The measurements along the foil length varied reproducibly by several percent. Attempts to correlate the variation of the magnetization with known thickness variations on a particular foil were only partially successful. Correcting for local thickness variations reduced the scatter of the magnetization data from an average of about 1.1% to 0.9%. All foils showed this variation along the foil length except for the 154 μm foils which had a scatter of 0.2%.

A subset of the previous foils were mounted in the final target frame. Each foil now had a dedicated pickup coil (500 turns) 16 mm in length. It was found that neighboring foils perturbed the foil out and foil in measurements by up to 1.5%. A downward systematic shift in the measured foil polarizations of 0.8% was observed compared to previous data with the 3 mm pickup coil.

A history of the polarization measurements made on the E–154 foils since 1993 is shown in Fig. 3. All polarizations are the average of measurements along the foil length. Measurements (1) were made in August of 1993 in the lab using a 3 mm long pickup coil with only one foil mounted inside the target assembly. Measurements (2) were made in the lab the following month with all foils in the final target frame. Each foil had a unique 16 mm long pick- up coil. Measurements (3) were made in May of 1994 after the E-143 run with the final frame and target assembly installed on the beam-line. All subsequent measurements were made on the beamline. Measurements (4) were made in July of 1995 prior to the E–154 data run. Measurements (5) were made in June of 1996 after the E–154 run. One of the 40 μ foils was new for E–154 The measurements before and after E–154 agree within 0.6 % with an average change of less than 0.1 %. The polarization of a few foils appear to have slightly degraded during the three years covered by this data, presumably from handling of the foils. The polarization values shown in Table 1 were calculated from the average of the measurements made before and after the E–154 run.

The overall error on the foil polarization is estimated as follows. The overall scale uncertainty from errors in g', foil composition, voltmeter calibration,

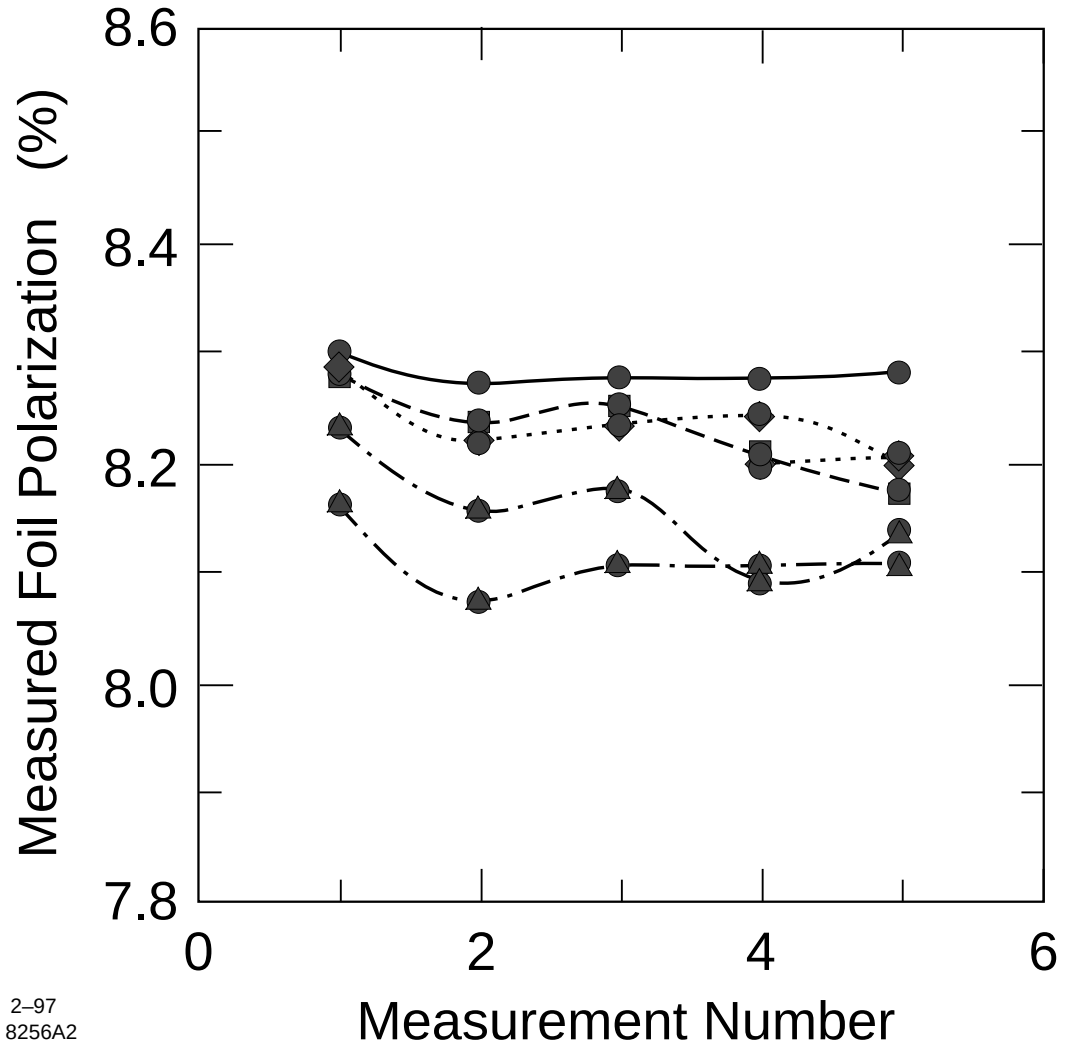

Fig. 3. Magnetization measurements of the E–154 target foils made at different times and conditions as described in the text. The lines connect measurements of the same foil and are coded as follows: solid line (154 μm), dotted line (40 μm), dashed line (30 μm), and dotdash line (20 μm).

length and mass is 0.7% . The spread of average foil polarizations for nominally identical foils of $0.9 - 1.3\%$ is used to bound the systematic measurement error. The remaining uncertainity is in the effect of neighboring foils (0.8)% and long term stability (0.2%). Adding in quadrature the above effects results in an overall relative systematic error of 1.7% .

3.5 Collimator, masking, and shielding

A collimating mask was placed 10.161 m from the target location before the spectrometer magnet. The mask, made from 25 radiation lengths of tung-

sten, had a central 45.7 mm diameter hole for the unscattered beam and two wedge-shaped holes to select vertically scattered electrons. The wedge-shaped openings gave a constant phi acceptance of 0.20 rad(top) and 0.22 rad(bottom) over the range of allowed scattering angles, $3.59 < \theta < 8.96$ mrad.

The Møller scattered electrons exited the collimator through .12 mm thick Al windows and then passed through air and helium bags while traveling through the magnet to the detector. A secondary Pb collimator located at the magnet face restricted the scattered rays to within ± 25 mm of the beam axis. As seen in Fig. 2, the beam pipe downstream of the magnet was shielded by a lead wall 5-10 cm thick. The combination of collimator, secondary masks, and shielding prevented single-bounce photons from the target from reaching the detector elements.

3.6 Magnet

A large aperture dipole spectometer magnet was located 12.40 m downstream of the target. To magnetically shield the beam from the dipole field a soft iron septum with a hole for the beam-pipe was centered in the magnet gap as shown in Fig. 2. The beamline was offset horizontally by 54 mm from the septum and magnet center.

The 3.0 m long dipole magnet typically operated at 900 A providing an integral $B \cdot dl$ of 33 kG-m. The magnetic field had both vertical and horizontal gradients of up to 0.5% per cm. Measurements of the $\int B_y dl$ with a Hall probe and two flip coils disagreed at the 0.7% level. A fit to the Hall probe data scaled by 0.9928 is used to calculate the average Møller momentum at the detectors. A systematic uncertainty of 0.7% is assigned to the momentum measurements.

The septum was 292 mm wide, 81 mm thick and 5 m long. The first meter of the septum was tapered to provide clearance for Møller scatters at 3.5 mrad. The septum, made from 1006 mild steel, had a 57 mm diameter hole for the beam to pass through. Inside the hole a mild steel beam-pipe with a 51 mm inner diameter provided additional magnetic shielding. At nominal currents the integral $B \cdot dl$ along the beam-line was 150 G-m.

3.7 Detectors

Five silicon detectors were mounted 28.90 m from the target behind 12.7 mm(bottom) or 19.1 mm(top) of lead in a lead lined detector hut as shown

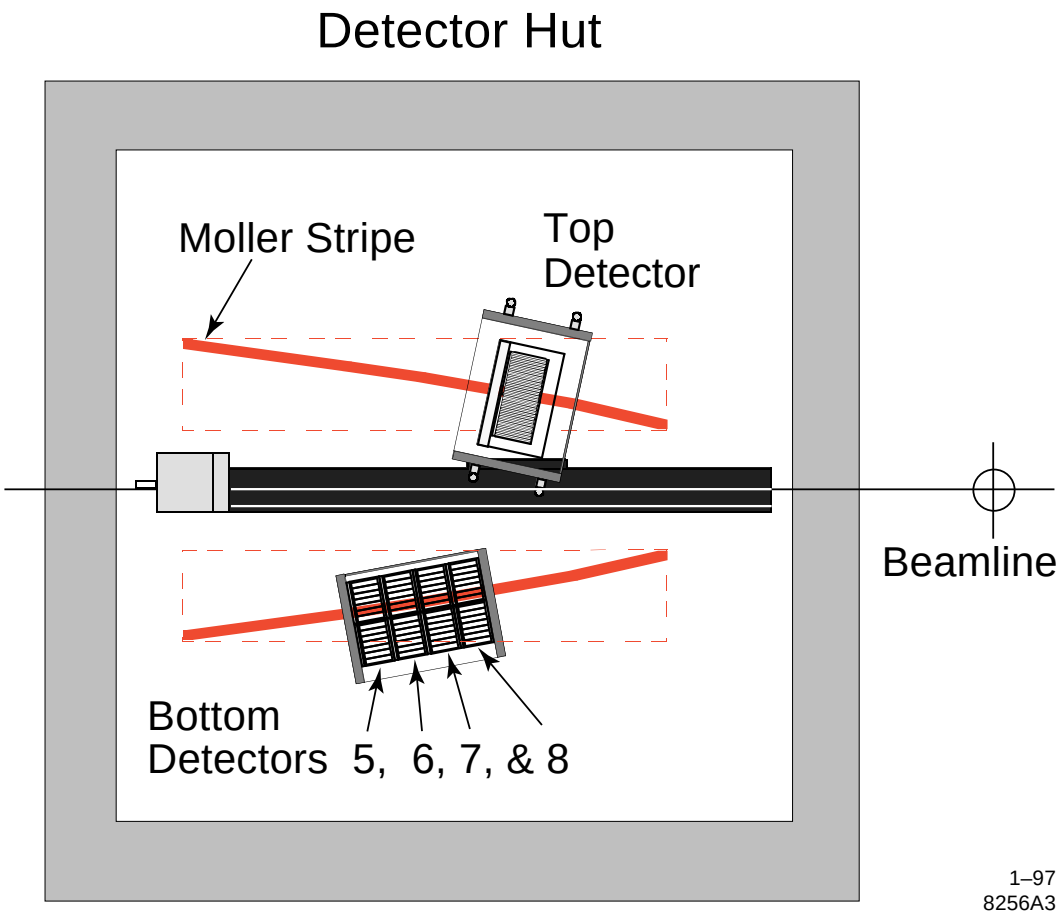

Fig. 4. The Møller detectors mounted inside the shielding hut. The top detector of 48 channels was mounted on a remotely controlled X-Y stage. The four bottom detectors, each with 12 channels, were mounted rigidly side by side.

in Fig. 4. Each detector contained two 4(x) by 6(y) cm silicon pad [3] devices approximately 300 μm thick. The top detector with 48 instrumented channels had a segmentation of 2.18 mm in the vertical (θ) direction. Each of the four bottom detectors had 12 instrumented channels 8.69 mm wide. The detectors were tilted by $+12.5°$(top) and $-10.2°$(bottom) to align the channels along the Møller scattered electron stripe.

The top detector was mounted on a remotely controlled X-Y stage and could be positioned anywhere within the Møller acceptance. The bottom four detectors were mounted rigidly side by side as a single unit. The bottom detector position was moved once during the run. Survey data before and after the E–154 data run confirm that positioning errors were less than 1 mm. Typically the Møller peak in the top detector was at x = 663 mm and y = 145 mm corresponding to scattering at 94° in the center of mass. The bottom detectors typically corresponded to scattering at center of mass angles of $93° - 104°$.

[3] Micron Semiconductor Ltd., Sussex, England.

The silicon channels were connected to 96 charge sensitive preamplifiers[9]. The preamplifiers integrated the signal over the 250 nsec beam spill. The preamplifier output was brought to the ESA counting house into SLAC-designed ADC's. The ADC's resided in E–154 beam CAMAC crates but were only read out during Møller runs. Linearity calibrations were made before and after the E–154 data run. Nonlinearities were less than 0.5% and typically less than 0.1% with the exception of one channel in the top detector which is not used in the present analysis.

4 Møller Data

The polarized electron beam was produced by photoemission from a strained GaAs photocathode illuminated with circularly polarized light from a flashlamp-pumped Ti-sapphire laser [10]. The light helcity was reversed randomly pulse by pulse. The beam helicity for each pulse was tagged by a right(R) or left(L) bit and this information was transmitted to the polarimeter. The beam was accelerated to 48.8 GeV/c and delivered to the experiment through SLAC beam-line A. The beam lost 400 Mev of energy due to synchrotron radiation before entering the end station. The electron spin rotates through 7.5 revolutions in the A-line thus reversing the beam helicity in the end station relative to the source.

Møller data were taken during special dedicated E–154 runs. Møller data taking required different beam optics from normal E–154 data taking. A quadrupole, between the Møller target and mask, had to be turned off. Upstream quads were then adjusted to maintain reasonable beam sizes. The Møller target was then positioned in the beam and the Møller magnet was turned on. Møller data runs were typically 10 minutes and yielded a statistical error of 0.001. Runs were usually taken in pairs with opposite polarity target fields. As the beam quality improved, systematic studies of the polarization dependence on the A-line beam energy and the source laser parameters were made. After the longitudinal beam polarization was optimized, the beam polarization was stable, changing significantly only when the beam current was altered.

5 Data Analysis

The Møller analysis proceeded through two steps. The first-pass analysis calculated average pulse heights and errors for each channel from the pulse by pulse data. Separate averages were made for pulses tagged by R and L polarization bits. Correlations between channels were calculated and recorded. A

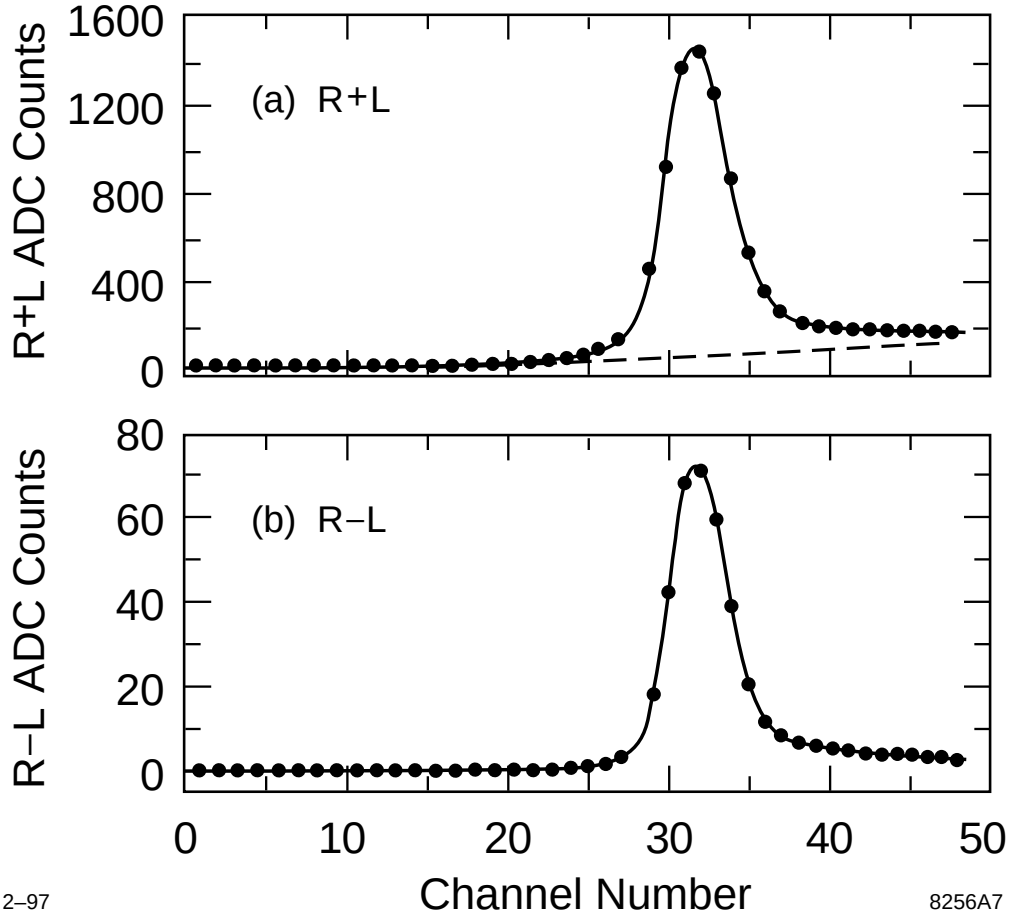

Fig. 5. The measured unpolarized (R+L) lineshape (a) and the polarized (R–L) lineshape (b) in the top detector are shown for a typical run. The dashed line is the fitted unpolarized background. The solid line is the fitted unpolarized Møller line-shape plus background.

very loose beam current requirement was made before including the pulse in the overall averages. A summary file containing the ADC averages, errors, and correlations, as well as useful beam and polarimeter parameters was written for each run.

A second-pass analysis read the summary file and formed sum (R+L) and difference (R–L) averages and errors for each channel. Typical (R+L) and (R–L) line-shapes for the top detector are shown in Fig. 5.

The background under the unpolarized (R+L) Møller scatters was estimated by fitting the (R+L) lineshape to an arbitrary quadratic background plus the lineshape expected from unpolarized Møller scattering. The technique for estimating the unpolarized lineshape used the observed R–L line-shape and the angular smearing functions shown in Fig. 1 to generate a predicted R+L line-shape for Møller scatters. The observed R+L distribution was then fit by this

predicted line-shape and a quadratic background. For zero target momenta the R–L line-shape and the R+L line-shapes are identical except for backgrounds. The trial R+L line-shape was generated from the observed R–L line-shape by first correcting for the angular smearing due to the polarized target electrons and then convoluting the result with the smearing correction for all (polarized and unpolarized) target electrons. Additional corrections were made for the variation of the cross section with scattering angle and for the variation in the value of the Møller scattering asymmetry over the angular acceptance of the detector. In an earlier experiment this technique was in excellent agreement with fits based on Monte Carlo generated line-shapes [4] which included the effects of the atomic motion of the target electrons [3] and multiple scattering and bremsstrahlung in the target foils and exit windows. The quadratic background and the overall fit are shown in Fig. 5.

An analyzing power for each detector was calculated from the target polarization and the expected Møller asymmetry. The expected asymmetry is a function of the beam energy and the average momentum of the Møller electrons in the peak. The momentum could be determined from the $\int B_y dl$ and the x position of the silicon channel containing the peak.

The measured asymmetry was calculated from the ADC averages by:

$$A_{meas.} = \frac{\sum_i (R-L)_i}{\sum_i (R+L)_i - \sum_i (BKG)_i}$$

where the sum is over the channels including the Møller peak. The sum range was chosen large enough to avoid the necessity of additional corrections for the target motion effect. The background subtraction increased the measured asymmetry by 17–24% . The statistical error in the sums was calculated using the correlation matrix between nearby channels.

6 Polarization Results and Study of Systematic Effects

A standard data set in which the beam polarization was stable for four weeks was used to study possible systematic errors in the polarization determination. Eight measurements each consisting of 2–6 Møller runs were made during this period. The calculated statistical error of the beam polarization determined by each detector per run ranged from 0.008 to 0.013. Combining the polarization data from the five detectors yielded a statistical precision of 0.004 to 0.006 per run. The polarization determined by each run was consistent with the measurement average within the statistical errors($< \chi^2/\mathrm{dof} >= 1.03$).

The average beam polarization of the standard data set was $P_z = 0.824 \pm 0.001$

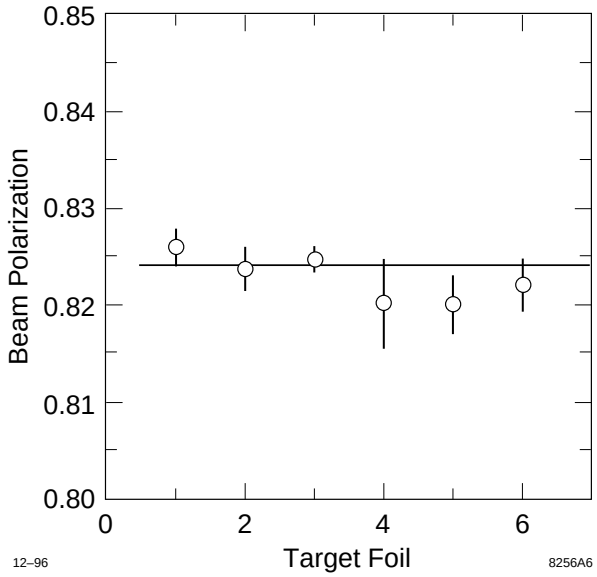

Fig. 6. Beam polarization determined from data using different target foils plotted versus the foil number as defined in Table 1. The solid line is a fit to the mean polarization.

(statistical error only). The spread of the polarization values determined by each measurement about the mean was slightly larger than that expected from statistical flucuations alone ($\chi^2 = 11.7$ for 7 dof) and may indicate that either the beam polarization or the polarimeter analyzing power changes with time. However, these effects are small, since a systematic fluctuation of only 0.002 per measurement would reduce the χ^2/dof to 1.0. A systematic uncertainity of 0.002 was added in quadrature to the statistical error of each measurement to account for these fluctuations.

6.1 Target Foil

As a check of the foil polarizations, the beam polarization determined by data from each target foil is shown in Fig. 6. The polarizations determined using each foil are in good agreement with each other and fit the common mean of 0.824 with a χ^2/dof $= 0.9$. If the foils were assumed to have identical polarizations instead of the measured values shown in Table 1, the χ^2/dof would increase to 5.4.

6.2 Beam Quality

The standard Møller first-pass analysis made only very loose cuts on the beam current per spill, rejecting typically 2.5% of the spills. To check the sensitivity

to potentially bad beam, ten runs were analyzed with tight cuts on beam current, beam quality, and beam position. Approximately 7.5% of the pulses were rejected by these cuts. No significant change in the measured polarization was seen.

6.3 Detector Dependence

The average beam polarization determined by each of the 5 detectors was calculated for runs with $\int B_y dl = 33$ kG-m. The polarizations so determined fit the common mean of 0.825 with a χ^2 of 9.7 for 4 dof. To investigate if the poor χ^2/dof was due to a systematic misalignment or error in $\int B_y dl$, the data was reanalyzed while varying $\int B_y dl$. It was found that a $\int B_y dl$ 1% lower than nominal reduced the spread in the polarization values determined from each detector to $\chi^2/\mathrm{dof} = 1$ while raising the mean to 0.827.

Alternatively, the 0.7% momentum uncertainty from the magnetic measurement data imply an average 0.3% uncertainty in the analyzing power of each detector. Adding this uncertainty in quadrature to the statistical error of the each detector would also result in a χ^2/dof of 1. To accomodate these findings, a 0.3% systematic error is assigned to the calculation of the detector analyzing power.

6.4 Range dependence

As described in the analysis section, the measured Møller asymmetry is determined by integrating (summing) the (R+L) and (R–L) pulse heights across the Møller peak. If the number of channels included in the integration range is too small, the asymmetry would be sensitive to the effects of the target electron atomic motion[3]. The sensitivity of the calculated asymmetry scaled by the detector analyzing power to the number of channels included in the integral is shown in Fig. 7. The present analysis uses 21 channels for the top detector and an equivalent number for the bottom detectors. A systematic uncertainty of 0.3% is assigned to the reflect the variation in the average beam polarization as the range is varied from 20 to 30 channels.

7 Systematic error

The overall systematic error has contributions from the foil polarization, uncertainties in the expected Møller asymmetry for each detector, and uncertainties

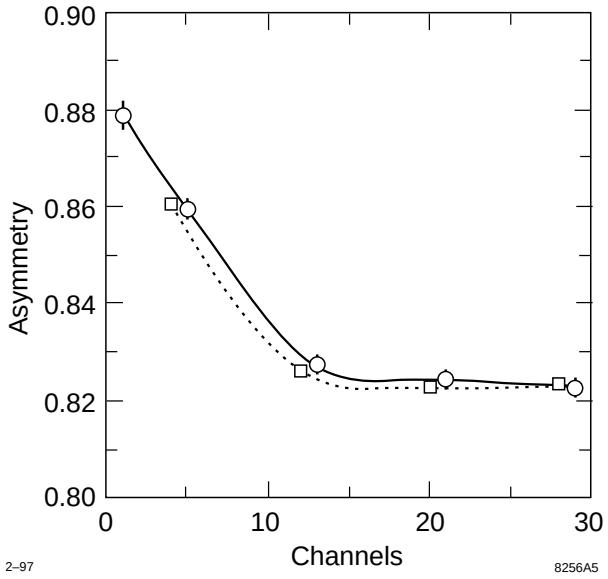

Fig. 7. Calculated asymmetry scaled by detector analyzing power determined by the top detector (solid curve) and average of the bottom detectors (dotted curve) plotted against the number of detector channels used in the sum over (R+L) and (R–L) data. The number of bottom channels is multiplied by 4 since the bottom channels are four times wider than the top.

in the background subtraction. The various contributions to the systematic error are summarized in Table 2.

The largest uncertainty is ascribed to the background correction which on average increases the raw asymmetry by 20% . As a check of the sensitivity of the calculated polarization to the shape of the background, the background was fit to several polynomial parameterizations. The (R+L) data were poorly fit by a linear background shape alone, requiring a second or higher order polynomial. The beam polarizations so determined varied by less than 1% relative when the background shape was varied from quadratic to quartic. To be conservative, the systematic error in the background correction is assumed to be double the observed 1% variation due to the background shape. Adding all systematic uncertainties in quadrature yields an overall relative systematic error of 2.7% .

8 Summary

A single arm Møller polarimeter used to measure the longitudinal polarization of a 48 GeV electron beam has been described. The data analysis procedure, including a correction for target atomic motion, and the target foil polarization determination has been discussed in detail. The polarimeter proved to be robust and stable. Consistent beam polarizations were obtained from six

Systematic error contribution	Value
Foil polarization	1.7%
Analyzing power	0.3%
Background correction	2.0%
Fit range	0.3%
TOTAL	2.7%

Table 2
Systematic error contributions to the beam polarization measurement.

different targets varying in thickness from 20 to 154μm and from 5 separate detectors collecting Møller scatters at $94 - 105^\circ$ in the center of mass. Statistical uncertainities of 0.002 per measurement made precision tests of possible systematic shifts in the data possible. Combining the systematic uncertainties lead to a final determination of the beam polarization with a relative uncertainity of 2.7%.

9 Acknowledgements

We gratefully ackowledge the help provided by the SLAC technical staff. In particular we would like to thank C. Hudspeth, J. Hrica, B. Sukiennicki, S. St. Lorant, and R. Arnold for their help in constructing the polarimeter. This work was supported by the U. S. Dept. of Energy contract DE-AC02-76ER00881(Wisconsin) and DE-AC03-76SF00515(SLAC).

References

[1] H. R. Band, AIP Conf. Proc. **343**, 245(1994).

[2] C. Møller, Ann. Phys. (Leipzig) **14**, 532(1932); J. Arrington *et al.*, Nucl. Instrum. Meth. **A311** 39(1992).

[3] L. G. Levchuk, Nucl. Instrum. Meth. **A345**, 496 (1994).

[4] M. Swartz, *et al.* Nucl. Instrum. Meth. **A363**, 526 (1995).

[5] M. J. Alguard *et al.,* Phys. Rev. Lett. **37**, 1261 (1976); *ibid.* **41**, 70 (1978).

[6] G. G. Scott and H. W. Sturner, Phys. Rev. **184**, 490 (1969).

[7] W. J. Carr, Phys. Rev. **85**, 590 (1952).).

[8] S. J. Barnett and G. S. Kenny, Phys. Rev. **87**, 723 (1952).

[9] R. Baggs *et al.* , Nucl. Instrum. Meth. **A344**, 547 (1994).

[10] T. Maruyama *et al.* , Phys. Rev. **B46**, 4261 (1992); R. Alley *et al.* , Nucl. Instrum. Meth. **A365**, 1 (1995).